Abiotic Acyl Transfer Cascades Driven by Aminoacyl Phosphate Esters and Self-Assembly

Mahesh D. Pol,[1,2] Ralf Thomann,[3,4] Yi Thomann,[3] and Charalampos G. Pappas[1,2*]

[1]DFG Cluster of Excellence *liv*MatS @FIT – Freiburg Center for Interactive Materials and Bioinspired Technologies, University of Freiburg, Georges-Köhler-Allee 105, 79110, Freiburg, Germany. [2]Institute of Organic Chemistry, University of Freiburg, Albertstrasse 21, 79104, Freiburg, Germany. [3]Freiburg Center for Interactive Materials and Bioinspired Technologies (FIT), University of Freiburg, Georges-Köhler-Allee 105, 79110, Freiburg, Germany. [4]Freiburg Materials Research Center (FMF), University of Freiburg, Stefan-Meier-Strasse 21, 79104, Freiburg, Germany.

ABSTRACT: Biochemical acyl transfer cascades, such as those initiated by the adenylation of carboxylic acids, are central to various biological processes, including protein synthesis and fatty acid metabolism. Designing aqueous cascades outside of biology remains challenging due to the need to control multiple, sequential reactions in a single pot and manage the stability of reactive intermediates. Herein, we developed abiotic cascades using aminoacyl phosphate esters, the synthetic counterparts of biological aminoacyl adenylates, to drive sequential chemical reactions and self-assembly in a single pot. We demonstrated that the structural elements of amino acid side chains (aromatic versus aliphatic) significantly influence the reactivity and half-lives of aminoacyl phosphate esters, ranging from hours to days. This behavior, in turn, affects the number of couplings we can achieve in the network and the self-assembly propensity of activated intermediate structures. The cascades are constructed using bifunctional peptide substrates featuring side chain nucleophiles. Specifically, aromatic amino acids facilitate the formation of transient thioesters, which preorganized into spherical aggregates and further couple into chimeric assemblies composed of esters and thioesters. In contrast, aliphatic amino acids, which lack the ability to form such structures, predominantly lead to hydrolysis, bypassing elongation after thioester formation. Additionally, in mixtures containing multiple aminoacyl phosphate esters and peptide substrates, we achieved selective product formation by following a distinct pathway that favors elongation through self-assembly. By coupling chemical reactions using molecules with varying reactivity timescales, we can drive multiple reaction clocks with distinct lifetimes and self-assembly dynamics, thereby facilitating precise temporal and structural regulation.

INTRODUCTION

Biochemical cascades[1-3] form intricate networks of pathways that sustain living processes through highly selective and regulated enzymatic reactions. A prime example is the activation of carboxylic acids by adenylation, which results in the formation of acyl adenylates.[4] In protein synthesis, aminoacyl adenylates (mixed phosphoric anhydrides of adenylic acid) transfer to tRNA molecules, forming ester bonds crucial for accurate and efficient peptide bond formation during translation.[5] The reactivity of aminoacyl adenylates also enables them to act as acyl donors in transesterification reactions, which is essential in fatty acid metabolism involving thioesters.[6] Similarly, luciferyl adenylates, formed by the catalysis of luciferin by luciferase enzymes, are key in the bioluminescence of organisms like fireflies and marine species.[7] Overall, these examples highlight the way in which structure and reactivity cross-regulate both primary and secondary metabolic processes.[8-10]

The complexity and efficiency of biochemical cascades have inspired chemists to develop fully synthetic systems that aim to replicate these processes.[11-13] However, achieving precise control and selectivity at every stage of transformation to prevent unwanted side reactions has been a significant challenge.[14] To address these challenges, systems chemistry[15-17] has emerged as a powerful tool, investigating the interactions and dynamics within chemical reaction networks.[18-21] This approach has proven highly effective in constructing complex self-assembling cascades[22-25] that involve diverse compound classes[26-27] and often incorporate biocatalysts.[28-32] Consequently, pathway-driven reconfigurations[33-37] have been utilized to impact the properties of these reaction networks, which are highly dependent on molecular architecture,[38-39] thermodynamic and kinetic parameters,[40-44] and assembly processes.[45-46]

Particularly in kinetically controlled assemblies,[47] reaction cycles[48-51] have been developed and further coupled with various functions such as self-assembly,[52-53] catalysis,[54-55] replication,[56-57] and responsiveness to external stimuli.[58-61] However, most of these systems

operate in a single step (assembly and disassembly).[62-66] The coupling of two chemical reaction cycles, in which the product of one cycle (an intermediate) serves as the substrate for a subsequent step and primarily influences the second coupling, remains rare. The reasons that remain rare are associated with the solubility and stability of activated building blocks in different environments, especially in water, which has a tendency to hydrolyze labile intermediates.

Herein, we design abiotic cascades driven by alterations in reactivity and self-assembly dynamics. In these systems, amino acyl phosphate esters, initially reconfigure to thioesters, leading to the formation of chimeric assemblies containing both ester and thioester functionalities in a single building block. These coupled chemical reactions are triggered by the structural elements surrounding the phosphoric anhydrides, where the amino acid side chains dictate the number of couplings and the self-assembly propensity. The activated amino acids bind covalently to bifunctional peptide substrates featuring side chain nucleophiles, giving rise to elongation or direct hydrolysis. We demonstrate that aminoacyl phosphate esters exhibit distinct reactivity patterns depending on whether they involve aliphatic or aromatic amino acid residues. This distinction impacts the stability, mechanical properties and structural arrangement of different types of activated amino acids within the cascades. Notably, we observed that when thioester formation occurs with aromatic amino acids, it leads to the fabrication of spherical aggregates, which then facilitate the formation of fibrous structures during subsequent coupling events. This process highlights the importance of thioester assembly in the initial reaction and the significance of intermolecular interactions, which were absent in phosphate esters containing aliphatic residues. Furthermore, when various aminoacyl phosphate esters compete for substrates, controlling reactivity and self-assembly enables the selective incorporation of residues into final structures that are capable of aggregation. Overall, these findings suggest that the structural elements surrounding activated amino acids can sequentially couple chemical reaction cycles in water through reactivity changes and self-assembly, without the need for complex enzymatic machinery.

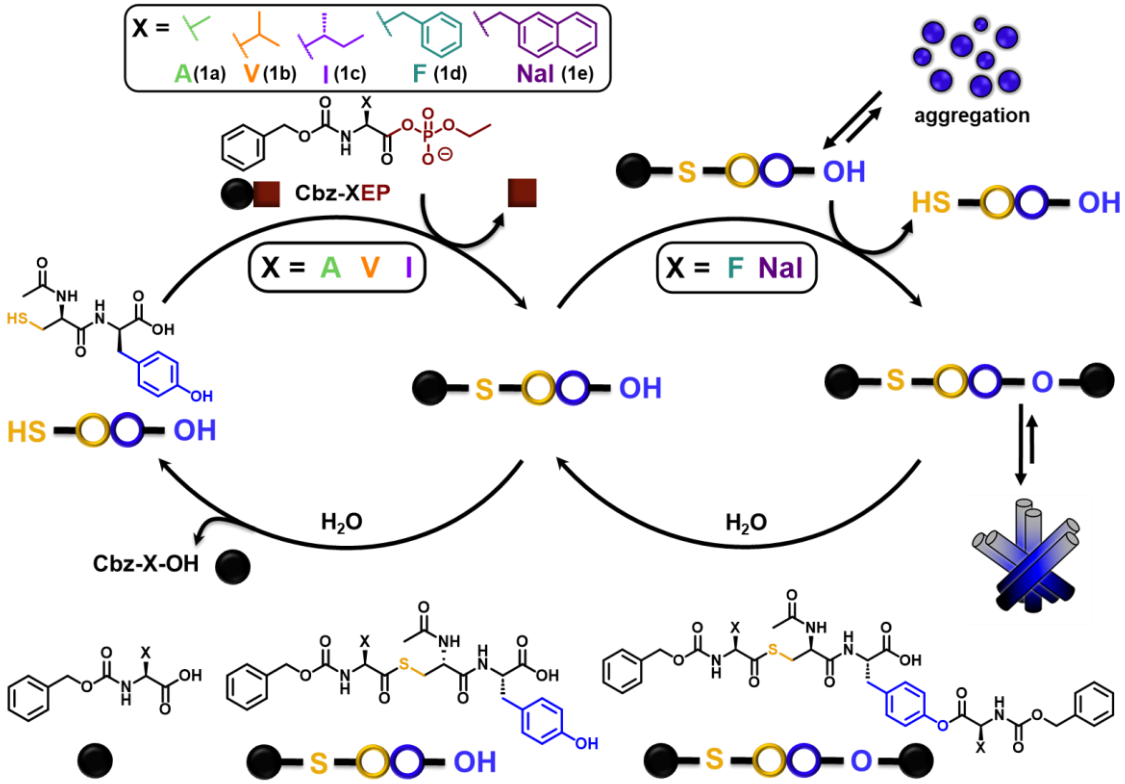

Figure 1. Schematic representation of the construction of abiotic cascades driven by the reaction between amino acyl phosphate esters (**Cbz-XEP**) and the dipeptide substrate **Ac-CY** (**2**) featuring cysteine and tyrosine residues. The reaction firstly proceeds though thioester formation, leading to the construction of chimeric structures composed of ester and thioester bonds. Aromatic amino acids within the structure of aminoacyl phosphate esters (**Cbz-FEP**, **Cbz-NalEP**) facilitate a second coupling step, where thioesters are capable of assembling into spherical aggregates. In contrast, aliphatic amino acid residues around the phosphate esters (**Cbz-AEP**, **Cbz-VEP** and **Cbz-IEP**) primarily lead to hydrolysis after thioester formation. Filled color spheres represent the amino acids in the structure of aminoacyl phosphate esters, while open spheres represent the amino acids in the structure of the dipeptide substrate.

RESULTS AND DISCUSSION

Design of acyl-driven abiotic cascades.

We have previously demonstrated that the amino acid side chains in the structure of aminoacyl phosphate esters dictated the length of the oligomers that were formed during spontaneous aminolytic reactions.[67] Additionally, the hydrophobicity of the amino acid side chains encoded the properties of transient assemblies upon covalent binding to substrates incorporating reactive nucleophiles.[68] These examples highlighted the way in which the structural elements around activated moieties (phosphoric anhydrides, esters or thioesters) guided reactivity changes, supramolecular structure formation and pathway selection. Herein, we focused on applying the concept of ''structured abiotic phosphates'' to the design and the construction of abiotic cascades in one pot. Thus, our objective was to fabricate systems where the structural elements in the structure of activated amino acids could: 1) impact the reactivity of intermediates, 2) couple chemical reaction in a single pot and 3) selectively switch on pathways as a result of self-assembly (Figure 1).

To achieve these goals and satisfy the criteria above, we utilized aminoacyl phosphate esters, which effectively solubilize hydrophobic amino acid derivatives in aqueous media. We incorporated aliphatic (alanine, valine, isoleucine), aromatic natural (phenylalanine), and non-natural amino acids (naphthylalanine) to investigate how reactivity is influenced by the chemical nature of the amino acid side chains (Supporting Table 1). The stability was investigated in different forms of C-terminus activated amino acid derivatives, including phosphoric anhydrides, thioesters and esters (Figure 2a). As a peptide substrate, we selected a short dipeptide sequence featuring cysteine and tyrosine residues, appended at the N-terminus with an acetyl group (**Ac-CY**) (Supporting Table 2). This bifunctional substrate allows us to study the competition between thioester and ester formation, as well as the self-assembly propensity of the different intermediates formed in the cascades.

Differential reactivity patterns from aminoacyl phosphate esters.

Building up from our previous observations on the reactivity of aminoacyl phosphate esters featuring an alanine residue (**Cbz-AEP**),[68] we sought to further investigate the hydrolysis trends by modifying the amino acid side chains with longer alkyl chains. Thus, we synthesized **Cbz-VEP** (**1b**) and **Cbz-IEP** (**1c**), using valine (**V**) and isoleucine (**I**) residues, respectively. We followed the same protocol for coupling and isolating the aminoacyl phosphate esters as described earlier.[67] Time-dependent Ultra Performance Liquid Chromatography (UPLC) experiments showed a significant increase in the stability of **Cbz-VEP** (**1b**) and **Cbz-IEP** (**1c**) compared to **Cbz-AEP** (**1a**) in 0.6 M borate buffer at pH 9.1. Specifically, **1b** exhibited a half-life of approximately 29 hours, while **1c** demonstrated an even longer half-life of 58 hours (Figure 2b and Supporting Table 3). In contrast, the half-life of **Cbz-AEP** (**1a**) was found to be around 3 hours. These results indicate that the introduction of bulky aliphatic side chains enhances the stability of aminoacyl phosphate esters due to steric hindrance, which protects the acyl phosphate ester bond from water hydrolysis. Moreover, the half-lives of **Cbz-FEP** (**1d**) and **Cbz-NalEP** (**1e**) was found to be around 1.5 hours. This demonstrates an inductive effect[64] from the aromatic amino acids, making the acyl carbon more electrophilic and, therefore, more susceptible to nucleophilic attack.

Next, we introduced the dipeptide substrate **Ac-CY** (**2**) into the systems, which contains nucleophilic groups from cysteine and tyrosine residues, facilitating the formation of thioester and ester bonds in tandem. The higher nucleophilicity of thiols enabled the initial formation of a thioester. Subsequently, the hydroxyl group of tyrosine facilitated the formation of ester bonds by performing a nucleophilic attack on the carbonyl group of the thioester (Figure 2a). We prepared samples by mixing various amino acyl phosphate esters (10 mM) with 10 mM **Ac-CY** (**2**) in 0.6 M borate buffer at pH 9.1. Specifically, in the cases of **1d** and **1e**, thioester formation occurred rapidly within 15 minutes, reaching a maximum conversion of around 8 mM. Notably, for **1b** and **1c**, maximum conversion occurred within 6 and 7 hours, respectively (Figure 2c). Despite the differences in the kinetics of thioester formation, relatively high yields were obtained in all samples, indicating that the amino acid side chains have a minimal effect on the yield of product formation during the first reaction. Subsequently, further intermolecular attack by the free hydroxyl group of tyrosine led to the formation of a di-ester, the second product of the reaction. The construction of this transient product (di-ester) in the second reaction varied significantly among the different samples. The highest yield was observed in the case of **1e**, reaching a maximum of 3.8 mM, whereas **1d** produced 2.4 mM. Aliphatic aminoacyl phosphate esters, such as **1a**, **1b** and **1c**, resulted in the formation of 0.25 mM, 0.7 mM, and 0.5 mM of the di-ester, respectively (Figures 2d and 2e). These observations highlight that the number of couplings in the cascade can be affected by chemical design (amino acid side chains). The reactivity and structural elements (aromatic *versus* aliphatic amino acid side chains) around the aminoacyl phosphate esters play a crucial role in determining the preferred pathway between elongation (second reaction) or direct hydrolysis. In order to confirm the selective coupling from the –**SH** group of the cysteine residue, we isolated the thioester peak from the reaction between **Cbz-FEP** (**1d**) and **Ac-CY** (**2**) using flash column chromatography. ^{1}H and ^{13}C NMR analysis confirmed that the coupling exclusively occurred due to

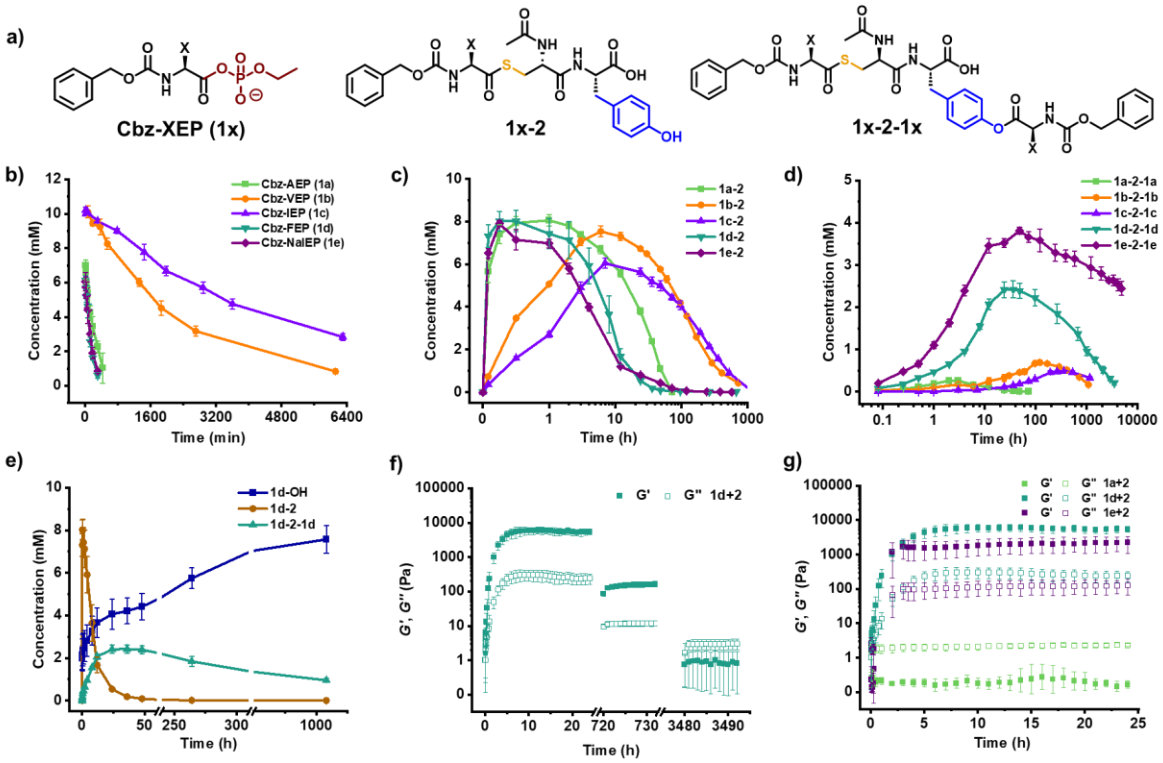

Figure 2. a) Chemical structure of aminoacyl phosphate esters (**1x**), thioester products (**1x-2**) in the first reaction and di-ester products in the second reaction. **b)** Hydrolysis profile of 10 mM **Cbz-AEP**, **Cbz-VEP**, **Cbz-IEP**, **Cbz-FEP** and **Cbz-NalEP** in 0.6 M borate buffer pH 9.1, analyzed using UPLC. **c)**, **d)** Time-dependent thioester and di-ester formation from the reaction between 10 mM **Cbz-XEP** (**X** = **A**, **V**, **I**, **F**, **Nal**) and 10 mM **Ac-CY** (**2**) in 0.6 M borate buffer pH 9.1. **e)** Time-dependent thioester and di-ester product formation of the reaction between 10 mM **1d** and 10 mM **2** in 0.6 M borate buffer pH 9.1.**1d-2** is shown with a different color compared to Figure 2c to avoid confusion. Storage and loss modulus as a function of time for the systems containing **f)** 10 mM **1d** and 10 mM **2**. **g)** 10 mM **1a**, **1d**, **1e** and 10 mM **2**. The solid squares represent the storage modulus (*G′*) and the open squares the loss modulus (*G″*). The thioester (**1d-2**) and di-ester (**1d-2-1d**) products presented in Figure 2e are the same as those presented in Figures 2c and 2d. They are added for a direct comparison with the rheology data. Similarly, in Figure 2g, the result of the mechanical properties of **1d** with **2** is reproduced from Figure 2f for comparison. In all graphs, error bars represent the standard deviation of three independent experiments conducted.

nucleophilic attack by the thiol group rather than the hydroxyl group of tyrosine. Additionally, from the same reaction mixture, we isolated the di-ester product and confirmed its structure using ^{1}H and ^{13}C NMR spectroscopy. The UPLC-MS analysis and kinetic profiles of all systems involving various aminoacyl phosphate esters (**XEPs**) with **Ac-CY** (**2**) are available in Supporting Information (Supporting Figures S1-S11).

Given that the second coupling occurred with a higher yield in the presence of aromatic amino acids, we investigated the concentration effects of aminoacyl phosphate esters in the cascade. We prepared samples of **1d** with **2** at different concentrations. Di-ester product formation was less efficient at lower concentrations, yielding 21% at 1 mM and 48% at 2.5 mM. However, at higher concentrations of 5 and 10 mM, di-ester yields increased to 58% and 64%, respectively (Supporting Figure S12). The increased yields at higher concentrations suggest an assembly event and a critical aggregation concentration required to efficiently promote the second coupling in the cascade. To further support these findings and highlight the importance of hydrophobic interactions in the second reaction, we prepared samples of **1d** and **1e** with **2** in a co-solvent mixture containing 20% acetonitrile (ACN). The yields of thioester formation (first reaction) were similar with and without the organic solvent. However, the yields of di-ester products were significantly lower, producing only 0.6 mM and 1.2 mM for **1d** and **1e**, respectively (Supporting Figure S13). These results indicate that self-assembly facilitates the coupling between the two reactions, and diminishing hydrophobic interactions minimizes the second coupling. In samples containing aliphatic aminoacyl phosphate esters, after thioester formation, we observed side reactions involving de-acetylation products (<0.6 mM) (Supporting Figures S14-S16).

Effect of self-assembly on cascade formation.
To further support the formation of aggregates, we performed continuous turbidity measurements for the reactions of **Cbz-XEPs** with **2** over a 24-hour period, monitoring the absorbance at 600 nm. These experiments confirmed a high aggregation propensity in case of **1d** and **1e**. In contrast, aminoacyl phosphate esters incorporating aliphatic amino acid side chains remained soluble throughout the entire 24-hour process (Supporting Figure S17). Using rheology, we found that the stiffness of the samples containing **1d** and **1e** was gradually enhanced, accompanied with the formation of hydrogels ($G' > G''$). Following the reaction of **1d** with **2** over time, we noticed that the stiffness was reduced and the system behaved as solution. This behaviour is attributed to the hydrolysis of the final transient ester products. The reaction of **1a** with **2** behaved like a liquid ($G'' > G'$) from the early stages of the reaction and remained unchanged until complete hydrolysis (Figure 2f and 2g). The structural organization at different stages of the reactions was monitored using cryo and negatively stained Transmission Electron Microscopy (TEM) experiments. TEM revealed distinct morphological differences between the assemblies formed by aminoacyl phosphate esters containing aromatic residues and those containing aliphatic residues.

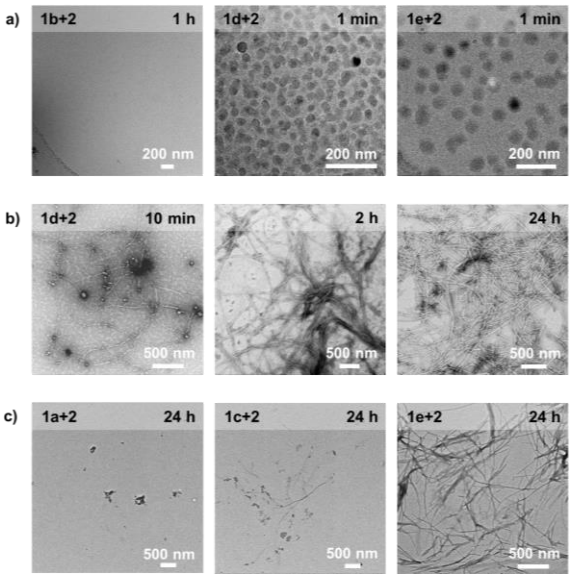

Figure 3. a) From left to right: Cryo-EM images of reactions involving 10 mM **Cbz-VEP** (**1b**), **Cbz-FEP** (**1d**) and **Cbz-NalEP** (**1e**) each with 10 mM **Ac-CY** (**2**), taken after 1 hour for **1b** and after 1 minute for **1d** and **1e**. To capture only the thioester structure, samples were analyzed by cryo-EM at the specified times, ensuring the presence of thioester but not di-ester. **b)** Time-dependent TEM images of the reaction between 10 mM **Cbz-FEP** (**1d**) and 10 mM **Ac-CY** (**2**). **c)** TEM images of reactions involving 10 mM **Cbz-XEP** (**1a**, **1c**, **1e**) and 10 mM **Ac-CY** (**2**) after 24 hours. All samples were prepared in 0.6 M borate buffer at pH 9.1.

Specifically, cryo-EM analysis of reactions between **1d** and **1e** with **2** revealed the formation of spherical aggregates during thioester formation (first reaction), while no structure was visualized for **1b** (Figure 3a). Subsequent reactions of **1d** and **1e** with **2**, showed a transformation into a dense fibrillar network, primarily consisting of the di-ester product. A progressive shortening of the fibers was noticed, which was associated with the hydrolysis of the di-ester product (Figure 3b and Supporting Figure S18). Furthermore, time-dependent TEM analysis showed that **1a** did not form any distinct assemblies when combined with **2** throughout the entire process (Figure 3c). However, fibrillar structures were observed for the di-ester products of **1b** and **1c**, indicating that more hydrophobic amino acids can form assemblies even at low concentrations of di-ester products (Supporting Figure S19).

To explore the effect of peptide sequence on the two distinct chemical reactions, we modified the initial sequence (**Ac-CY**) by introducing an anionic (aspartic acid, **D**) and an aliphatic (valine, **V**) amino acid residue at the C-terminus. Our aim was to evaluate the impact of these C-terminal modifications on the yields of thioester and di-ester products, considering both kinetic and assembly effects derived from the chemical structure of the tripeptide substrates. We used **1d** and **1e** due to their high reactivity and propensity to form assemblies upon transferring the aromatic amino acids into the new activated forms (thioesters and esters). From the reactions of **1d** and **1e** with **Ac-CYD** (**3**), we observed lower yields for both thioester and di-ester products compared to **Ac-CY** (**2**). Specifically, the reaction of **1d** with **3** produced 7.4 mM of thioester and 1.2 mM of di-ester, while **1e** with **3** yielded 6.4 mM and 3.4 mM, respectively. When replacing **Ac-CYD** (**3**) with **Ac-CYV** (**4**), we observed higher yields for the products of both reactions, which were similar to those produced using **Ac-CY** (Supporting Figures S20-S29). TEM analysis provided insights into the structural reconfigurations over time. Upon mixing **1e** with **3**, an initial non-defined assembly was observed during thioester formation. However, after the second coupling, a dense fibrillar network formed due to the high yield of di-ester formation. In the tripeptide sequence involving valine residues, fibers and ribbon-like assemblies were observed (Supporting Figure S30). These results suggest that incorporating anionic residues at the C-terminus of the tripeptide substrates influences product yields in both reactions, by affecting the self-assembly propensity of the intermediates formed.

Selective coupling in abiotic cascade networks.
In order to investigate the competition between phosphate esters and substrates in cascade formation, we conducted experiments using various mixtures. The mixtures included combinations of **1d/1b** with **2** and

1e/**1b** with **2**, combining two activated amino acids with one peptide substrate (Figure 4a upper panel). The selection of **1d**, **1e** and **1b** was based on their differing reactivity and propensity to form the second coupling product. Additionally, we aimed to explore whether co-assembly effects between the activated amino acids could influence the efficiency of thioester and di-ester formation, particularly for aliphatic amino acid residues, which typically showed lower coupling yields. Notably, in the mixture containing **1e**/**1b** and **2**, we observed the formation of 3.9 mM of thioester from **1e**, which is significantly higher compared to the 0.4 mM formed from **1b**. The thioester from **1e** further converted into 3.3 mM of its di-ester product (Figure 4b). Similarly, in the mixture containing **1d**/**1b** and **2**, **1d** produced 3.8 mM of thioester, which subsequently converted to 1.5 mM of the di-ester product (Supporting Figures S31-S35). These results indicate that mixtures containing aminoacyl phosphate esters with different reactivity patterns (aromatic *versus* aliphatic residues) can selectively form di-ester products. This selective formation incorporates aromatic amino acids from the phosphate esters into the final chimeric structures.

Additionally, we conducted experiments by mixing **1d** or **1e** with two tripeptide substrates, **Ac-CYD** (**3**) and **Ac-CYV** (**4**) in a single pot. Our aim was to investigate the way in which the tripeptide sequences influence the selective formation of products in the cascade, when they are incorporated into the activated amino acids in both reactions (Figure 4a lower panel). Upon mixing **1e** with **3** and **4**, we observed the formation of 3.3 mM thioester with **3** and 5.4 mM with **4**. In the second reaction, the di-ester product primarily formed from **4**, reaching a maximum yield of 2.6 mM. In contrast, the second coupling product with **3** resulted in a significantly lower yield of only 0.3 mM (Figure 4c). Similarly, in the reaction of **1d** with **3** and **4**, we observed a comparable trend, with di-ester product formation being significantly more pronounced with peptide **4** (Supporting Figures S36-S40). These findings highlight the important role of specific amino acids within tripeptide substrates in influencing efficiency and selectivity within the cascades. Notably, our approach demonstrates the ability to incorporate peptide sequences containing nucleophiles, irrespective of their length. This capability has been effectively observed in both dipeptides and

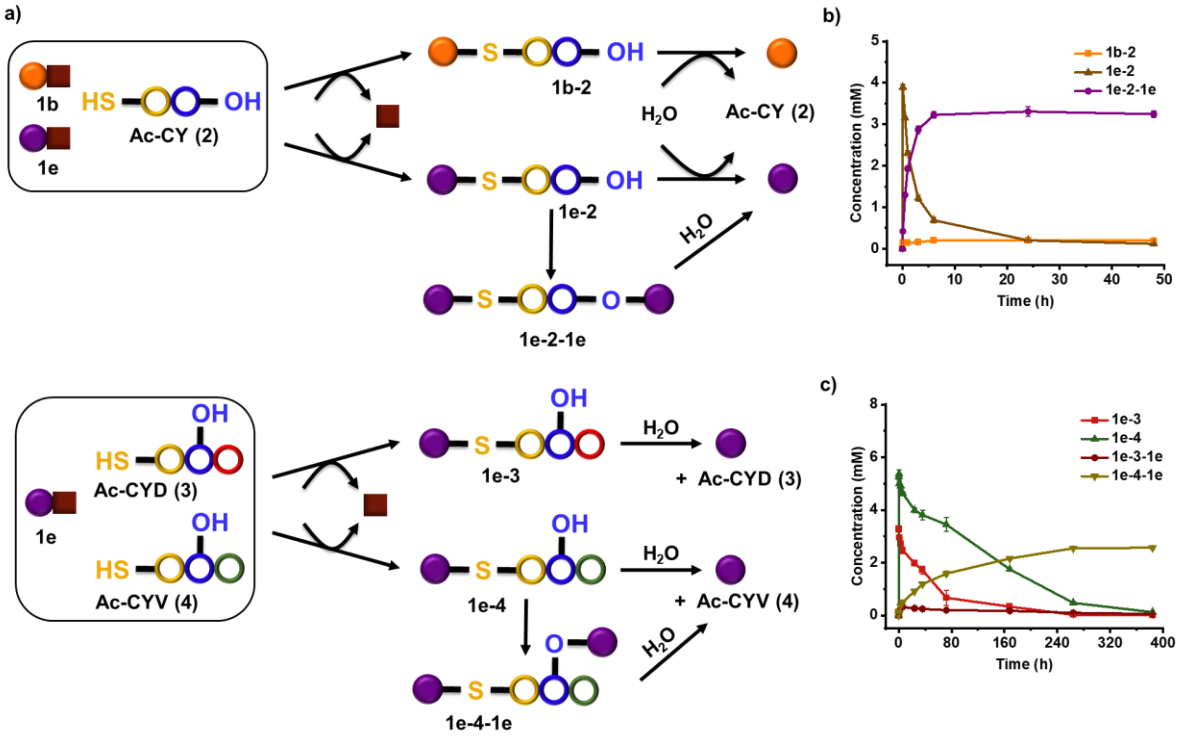

Figure 4. a) Schematic representation of different species formed in mixtures containing two aminoacyl phosphate esters (**1b**, **1e**) and the bifunctional dipeptide substrate (**2**), as well as one aminoacyl phosphate ester (**1e**) and two bifunctional tripeptide substrates (**3**, **4**), leading to the selective formation of di-ester products. To avoid confusion, we used different color coding for valine in the tripeptide substrate (**4**) distinct from that used for the valine in the aminoacyl phosphate ester (**1b**). Time-dependent formation of thioester and di-ester products in samples containing a mixture of **b)** 10 mM **Cbz-VEP** (**1b**), 10 mM **Cbz-NalEP** (**1e**), and 5 mM **Ac-CY** (**2**) in 0.6 M borate buffer at pH 9.1, and **c)** 10 mM **Cbz-NalEP** (**1e**), 10 mM **Ac-CYD** (**3**) and 10 mM **Ac-CYV** (**4**) in 0.6 M borate buffer at pH 9.1. Error bars represent the standard deviation of three independent experiments conducted.

tripeptides, which guided cascade formation. Detailed reaction pathways for the mixtures containing three components are available in the supporting information (Supporting Figures S41 and S42).

CONCLUSIONS

In this work, we focused on constructing abiotic cascades by influencing the reactivity and self-assembly dynamics of acyl transfer reactions initiated by aminoacyl phosphate esters. We demonstrated that the structural elements surrounding phosphate esters can modulate their reactivity and half-lives, ranging from hours for aromatic amino acids to days for aliphatic residues. This variability in turn dictates reaction pathways and influences the propensity for self-assembly when the structural elements (amino acid side chains) are transferred into other activated forms, such as esters and thioesters. Aminoacyl phosphate esters containing aromatic residues facilitated a two-step coupling process, initially forming thioesters capable of assembling into spherical aggregates. This process enabled the fabrication of chimeric assemblies incorporating both ester and thioester bonds within a single structure. Conversely, activated amino acids with aliphatic residues predominantly underwent hydrolysis after thioester formation. Furthermore, we achieved selective product formation in complex mixtures containing aminoacyl phosphate esters and peptide substrates by leveraging self-assembly as a selection mechanism to influence cascade formation. By promoting or inhibiting specific pathways based on structural elements and assembly dynamics, we enhanced both the efficiency and specificity of the reactions. Our approach demonstrates how the interplay between assembly and reactivity enables the coupling of chemical reactions within a single-step process. In future, we will focus on further understanding how minimal changes in the structure of amino acid side chains can affect reactivity and influence non-equilibrium cascade formation. Coupling chemical reaction cycles through self-assembly, with the potential incorporation of chemical shunts[19], presents a novel opportunity to direct orthogonal functions within chemical reaction networks.

ASSOCIATED CONTENT

Supporting Information

The Supporting Information is available free of charge on the ACS Publications website. The Supporting Information contains a Materials and Methods description and additional UPLC chromatograms, LC-MS analyses, kinetic profiles, reaction pathways, tables with chemical structures, Transmission Electron Microscopy images and turbidity measurements.

Data availability. The data that support the findings of this study are available from the corresponding author upon reasonable request.

AUTHOR INFORMATION

Corresponding Author

*charalampos.pappas@livmats.uni-freiburg.de

Funding Sources

The work was supported by the Deutsche Forschungsgemeinschaft (DFG, German Research Foundation) under Germany's Excellence Strategy – EXC-2193/1 – 390951807 and the European Union (ERC-2023-StG grant, PhosphotoSupraChem, 101117240).

ACKNOWLEDGMENTS

We thank Christoph Warth for analytical support.

REFERENCES

1. Wheeldon, I.; Minteer, S. D.; Banta, S.; Barton, S. C.; Atanassov, P.; Sigman, M., Substrate channelling as an approach to cascade reactions. *Nat. Chem.* **2016**, *8* (4), 299-309.
2. Saini, K.; Discher, D. E., Forced Unfolding of Proteins Directs Biochemical Cascades. *Biochemistry* **2019**, *58* (49), 4893-4902.
3. Alam-Nazki, A.; Krishnan, J., Spatial Control of Biochemical Modification Cascades and Pathways. *Biophys. J.* **2015**, *108* (12), 2912-24.
4. Nguyen, H. T.; Lee, S.; Shin, K., Controlled metabolic cascades for protein synthesis in an artificial cell. *Biochem. Soc. Trans.* **2021**, *49* (5), 2143-2151.
5. Trobro, S.; Aqvist, J., Mechanism of peptide bond synthesis on the ribosome. *Proc. Natl. Acad. Sci. U. S. A.* **2005**, *102* (35), 12395-400.
6. Franke, J.; Hertweck, C., Biomimetic Thioesters as Probes for Enzymatic Assembly Lines: Synthesis, Applications, and Challenges. *Cell. Chem. Biol.* **2016**, *23* (10), 1179-1192.
7. Conti, E.; Franks, N. P.; Brick, P., Crystal structure of firefly luciferase throws light on a superfamily of adenylate-forming enzymes. *Structure* **1996**, *4* (3), 287-98.
8. Das, K.; Gabrielli, L.; Prins, L. J., Chemically Fueled Self-Assembly in Biology and Chemistry. *Angew. Chem. Int. Ed.* **2021**, *60*, 20120 – 20143.
9. Chatterjee, A.; Reja, A.; Pal, S.; Das, D., Systems chemistry of peptide-assemblies for biochemical transformations. *Chem. Soc. Rev.* **2022**, *51* (8), 3047-3070.
10. Otto, S., An Approach to the De Novo Synthesis of Life. *Acc. Chem. Res.* **2022**, *55* (2), 145-155.
11. Aida, T.; Meijer, E. W.; Stupp, S. I., Functional supramolecular polymers. *Science* **2012**, *335* (6070), 813-7.
12. Lehn, J. M., Toward complex matter: supramolecular chemistry and self-organization. *Proc. Natl. Acad. Sci. U. S. A.* **2002**, *99* (8), 4763-8.
13. Borsley, S.; Leigh, D. A.; Roberts, B. M. W., Molecular Ratchets and Kinetic Asymmetry: Giving Chemistry Direction. *Angew. Chem. Int. Ed.* **2024**, *63* (23), e202400495.
14. Wang, C.; Yue, L.; Willner, I., Controlling biocatalytic cascades with enzyme-DNA dynamic networks. *Nat. Catal.* **2020**, *3* (11), 941-950.
15. Ashkenasy, G.; Hermans, T. M.; Otto, S.; Taylor, A. F., Systems chemistry. *Chem. Soc. Rev.* **2017**, *46* (9), 2543-2554.
16. Vantomme, G.; Meijer, E. W., The construction of supramolecular systems. *Science* **2019**, *363* (6434), 1396-1397.
17. Sheehan, F.; Sementa, D.; Jain, A.; Kumar, M.; Tayarani-Najjaran, M.; Kroiss, D.; Ulijn, R. V., Peptide-Based Supramolecular Systems Chemistry. *Chem. Rev.* **2021**, 121 (22), 13869-13914.

18. Deng, J.; Walther, A., Autonomous DNA nanostructures instructed by hierarchically concatenated chemical reaction networks. *Nat. Commun.* **2021**, *12* (1), 5132.
19. Sharko, A.; Spitzbarth, B.; Hermans, T. M.; Eelkema, R., Redox-Controlled Shunts in a Synthetic Chemical Reaction Cycle. *J. Am. Chem. Soc.* **2023**, *145* (17), 9672-9678.
20. Maguire, O. R.; Smokers, I. B. A.; Oosterom, B. G.; Zheliezniak, A.; Huck, W. T. S., A Prebiotic Precursor to Life's Phosphate Transfer System with an ATP Analog and Histidyl Peptide Organocatalysts. *J. Am. Chem. Soc.* **2024**, *146* (11), 7839-7849.
21. Gabrielli, L.; Goldin, L.; Chandrabhas, S.; Dalla Valle, A.; Prins, L. J., Chemical Information Processing by a Responsive Chemical System. *J. Am. Chem. Soc.* **2024**, *146* (3), 2080-2088.
22. Campbell, V. E.; de Hatten, X.; Delsuc, N.; Kauffmann, B.; Huc, I.; Nitschke, J. R., Cascading transformations within a dynamic self-assembled system. *Nat. Chem.* **2010**, *2* (8), 684-7.
23. Chatterjee, A.; Mahato, C.; Das, D., Complex Cascade Reaction Networks via Cross beta Amyloid Nanotubes. *Angew. Chem. Int. Ed.* **2021**, *60* (1), 202-207.
24. Dhasaiyan, P.; Ghosh, T.; Lee, H. G.; Lee, Y.; Hwang, I.; Mukhopadhyay, R. D.; Park, K. M.; Shin, S.; Kang, I. S.; Kim, K., Cascade reaction networks within audible sound induced transient domains in a solution. *Nat. Commun.* **2022**, *13* (1), 2372.
25. Fu, H.; Pramanik, S.; Aprahamian, I., Metal and Proton Relay-Controlled Hierarchical Multistep Switching Cascade. *J. Am. Chem. Soc.* **2023**, *145* (36), 19554-19560.
26. Kroll, S.; Niemeyer, C. M., Nucleic Acid-based Enzyme Cascades-Current Trends and Future Perspectives. *Angew. Chem. Int. Ed.* **2024**, *63* (5), e202314452.
27. Bianco, S.; Hasan, M.; Ahmad, A.; Richards, S. J.; Dietrich, B.; Wallace, M.; Tang, Q.; Smith, A. J.; Gibson, M. I.; Adams, D. J., Mechanical release of homogenous proteins from supramolecular gels. *Nature* **2024**, *631* (8021), 544-548.
28. Sahoo, J. K.; Pappas, C. G.; Sasselli, I. R.; Abul-Haija, Y. M.; Ulijn, R. V., Biocatalytic Self-Assembly Cascades. *Angew. Chem. Int. Ed.* **2017**, *56* (24), 6828-6832.
29. Walsh, C. T.; Moore, B. S., Enzymatic Cascade Reactions in Biosynthesis. *Angew. Chem. Int. Ed.* **2019**, 58 (21), 6846-6879.
30. Ghosh, S.; Baltussen, M. G.; Ivanov, N. M.; Haije, R.; Jakstaite, M.; Zhou, T.; Huck, W. T. S., Exploring Emergent Properties in Enzymatic Reaction Networks: Design and Control of Dynamic Functional Systems. *Chem. Rev.* **2024**, 124 (5), 2553-2582.
31. Reja, A.; Afrose, S. P.; Das, D., Aldolase Cascade Facilitated by Self-Assembled Nanotubes from Short Peptide Amphiphiles. *Angew. Chem. Int. Ed.* **2020**, *59* (11), 4329-4334.
32. Wilner, O. I.; Weizmann, Y.; Gill, R.; Lioubashevski, O.; Freeman, R.; Willner, I., Enzyme cascades activated on topologically programmed DNA scaffolds. *Nat. Nanotechnol.* **2009**, *4* (4), 249-54.
33. Korevaar, P. A.; Schaefer, C.; de Greef, T. F.; Meijer, E. W., Controlling chemical self-assembly by solvent-dependent dynamics. *J. Am. Chem. Soc.* **2012**, *134* (32), 13482-91.
34. Paul, S.; Gayen, K.; Cantavella, P. G.; Escuder, B.; Singh, N., Complex Pathways Drive Pluripotent Fmoc-Leucine Self-Assemblies. *Angew. Chem. Int. Ed.* **2024**, e202406220.
35. Deng, J.; Walther, A., Pathway Complexity in Fuel-Driven DNA Nanostructures with Autonomous Reconfiguration of Multiple Dynamic Steady States. *J. Am. Chem. Soc.* **2020**, *142* (2), 685-689.
36. Mishra, A.; Korlepara, D. B.; Balasubramanian, S.; George, S. J., Bioinspired, ATP-driven co-operative supramolecular polymerization and its pathway dependence. *Chem. Commun.* **2020**, *56* (10), 1505-1508.
37. Pappas, C. G.; Sasselli, I. R.; Ulijn, R. V., Biocatalytic Pathway Selection in Transient Tripeptide Nanostructures. *Angew. Chem. Int. Ed.* **2015**, *54* (28), 8119-23.
38. Jacobs, W. M.; Reinhardt, A.; Frenkel, D., Rational design of self-assembly pathways for complex multicomponent structures. *Proc. Natl. Acad. Sci. U. S. A.* **2015**, *112* (20), 6313-8.
39. Ghosh, G., Pathway dependent controlled supramolecular polymerization of peptides. *Giant* **2023**, 14.
40. Luan, J.; Wang, D.; Zhang, S.; Miyazaki, Y.; Shinoda, W.; Wilson, D. A., Complex Energy Landscapes of Self-Assembled Vesicles. *J. Am. Chem. Soc.* **2023**, *145* (28), 15496-15506.
41. Wang, J.; Liu, K.; Xing, R.; Yan, X., Peptide self-assembly: thermodynamics and kinetics. *Chem. Soc. Rev.* **2016**, *45* (20), 5589-5604.
42. Tantakitti, F.; Boekhoven, J.; Wang, X.; Kazantsev, R. V.; Yu, T.; Li, J.; Zhuang, E.; Zandi, R.; Ortony, J. H.; Newcomb, C. J.; Palmer, L. C.; Shekhawat, G. S.; de la Cruz, M. O.; Schatz, G. C.; Stupp, S. I., Energy landscapes and functions of supramolecular systems. *Nat. Mater.* **2016**, *15* (4), 469-76.
43. Laishram, R.; Sarkar, S.; Seth, I.; Khatun, N.; Aswal, V. K.; Maitra, U.; George, S. J., Secondary Nucleation-Triggered Physical Cross-Links and Tunable Stiffness in Seeded Supramolecular Hydrogels. *J. Am. Chem. Soc.* **2022**, *144* (25), 11306-11315.
44. Aprahamian, I.; Goldup, S. M., Non-equilibrium Steady States in Catalysis, Molecular Motors, and Supramolecular Materials: Why Networks and Language Matter. *J. Am. Chem. Soc.* **2023**, *145* (26), 14169-14183.
45. Yin, P.; Choi, H. M.; Calvert, C. R.; Pierce, N. A., Programming biomolecular self-assembly pathways. *Nature* **2008**, *451* (7176), 318-22.
46. Fu, H. L.; Huang, J. Y.; van der Tol, J. J. B.; Su, L.; Wang, Y. Y.; Dey, S.; Zijlstra, P.; Fytas, G.; Vantomme, G.; Dankers, P. Y. W.; Meijer, E. W., Supramolecular polymers form tactoids through liquid-liquid phase separation. *Nature* **2024**, *626* (8001).
47. Ouyang, Y.; Zhang, P.; Willner, I., Dissipative biocatalytic cascades and gated transient biocatalytic cascades driven by nucleic acid networks. *Sci. Adv.* **2022**, *8* (18), eabn3534.
48. Mitchison, T.; Kirschner, M., Dynamic instability of microtubule growth. *Nature* **1984**, *312* (5991), 237-242.
49. Borsley, S.; Leigh, D. A.; Roberts, B. M. W., Chemical fuels for molecular machinery. *Nat. Chem.* **2022**, *14* (7), 728-738.
50. Sharko, A.; Livitz, D.; De Piccoli, S.; Bishop, K. J. M.; Hermans, T. M., Insights into Chemically Fueled Supramolecular Polymers. *Chem. Rev.* **2022**, *122* (13), 11759-11777.
51. De, S.; Klajn, R., Dissipative Self-Assembly Driven by the Consumption of Chemical Fuels. *Adv. Mater.* **2018**, *30* (41), e1706750.
52. Zozulia, O.; Kriebisch, C. M. E.; Kriebisch, B. A. K.; Soria-Carrera, H.; Ryadi, K. R.; Steck, J.; Boekhoven, J., Acyl Phosphates as Chemically Fueled Building Blocks for Self-Sustaining Protocells. *Angew. Chem. Int. Ed.* **2024**, *63* (30), e202406094.
53. Shandilya, E.; Rallabandi, B.; Maiti, S., In situ enzymatic control of colloidal phoresis and catalysis through hydrolysis of ATP. *Nat. Commun.* **2024**, *15* (1), 3603.
54. Al Shehimy, S.; Le, H. D.; Amano, S.; Di Noja, S.; Monari, L.; Ragazzon, G., Progressive endergonic synthesis of Diels-Alder adducts driven by chemical energy. *Angew. Chem. Int. Ed.* **2024**, e202411554.
55. Olivieri, E.; Gallagher, J. M.; Betts, A.; Mrad, T. W.; Leigh, D. A., Endergonic synthesis driven by chemical fuelling. *Nat. Synth.* **2024**, *3* (6), 707-714.

56. Howlett, M. G.; Engwerda, A. H. J.; Scanes, R. J. H.; Fletcher, S. P., An autonomously oscillating supramolecular self-replicator. *Nat. Chem.* **2022**, *14* (7), 805-810.
57. Paikar, A.; Novichkov, A. I.; Hanopolskyi, A. I.; Smaliak, V. A.; Sui, X.; Kampf, N.; Skorb, E. V.; Semenov, S. N., Spatiotemporal Regulation of Hydrogel Actuators by Autocatalytic Reaction Networks. *Adv. Mater.* **2022**, *34* (13), e2106816.
58. Hwang, I.; Mukhopadhyay, R. D.; Dhasaiyan, P.; Choi, S.; Kim, S. Y.; Ko, Y. H.; Baek, K.; Kim, K., Audible sound-controlled spatiotemporal patterns in out-of-equilibrium systems. *Nat. Chem.* **2020**, *12* (9), 808-813.
59. Wu, J.; Greenfield, J. L., Photoswitchable Imines Drive Dynamic Covalent Systems to Nonequilibrium Steady States. *J. Am. Chem. Soc.* **2024**.
60. Weissenfels, M.; Gemen, J.; Klajn, R., Dissipative Self-Assembly: Fueling with Chemicals versus Light. *Chem* **2021**, *7* (1), 23-37.
61. Lang, X.; Huang, Y.; He, L.; Wang, Y.; Thumu, U.; Chu, Z.; Huck, W. T. S.; Zhao, H., Mechanosensitive non-equilibrium supramolecular polymerization in closed chemical systems. *Nat. Commun.* **2023**, *14* (1), 3084.
62. Del Giudice, D.; Di Stefano, S., Dissipative Systems Driven by the Decarboxylation of Activated Carboxylic Acids. *Acc. Chem. Res.* **2023**, *56* (7), 889-899.
63. Olivieri, E.; Quintard, G.; Naubron, J.-V.; Quintard, A., Chemically Fueled Three-State Chiroptical Switching Supramolecular Gel with Temporal Control. *J. Am. Chem. Soc.* **2021**, *143* (32), 12650-12657.
64. Englert, A.; Majer, F.; Schiessl, J. L.; Kuehne, A. J. C.; von Delius, M., Acylphosphates as versatile transient species in reaction networks and optical catalyst screenings. *Chem* **2024**, 10, 1–14
65. Kariyawasam, L. S.; Hossain, M. M.; Hartley, C. S., The Transient Covalent Bond in Abiotic Nonequilibrium Systems. *Angew. Chem. Int. Ed.* **2021**, *60* (23), 12648-12658.
66. Jones, G. R.; Wang, H. S.; Parkatzidis, K.; Whitfield, R.; Truong, N. P.; Anastasaki, A., Reversed Controlled Polymerization (RCP): Depolymerization from Well-Defined Polymers to Monomers. *J. Am. Chem. Soc.* **2023**, *145* (18), 9898-9915.
67. Dai, K.; Pol, M. D.; Saile, L.; Sharma, A.; Liu, B.; Thomann, R.; Trefs, J. L.; Qiu, D.; Moser, S.; Wiesler, S.; Balzer, B. N.; Hugel, T.; Jessen, H. J.; Pappas, C. G., Spontaneous and Selective Peptide Elongation in Water Driven by Aminoacyl Phosphate Esters and Phase Changes. *J. Am. Chem. Soc.* **2023**, *145*, 48, 26086–26094.
68. Pol, M. D.; Dai, K.; Thomann, R.; Moser, S.; Kanti Roy, S.; Pappas, C. G., Guiding Transient Peptide Assemblies with Structural Elements Embedded in Abiotic Phosphate Fuels. *Angew. Chem. Int. Ed.* **2024**, *63* (28), e202404360.

TOC